Characterization of Low-Energy Chlorophylls in the PSI-LHCI Supercomplex from *Chlamydomonas reinhardtii*. A Site-Selective Fluorescence Study

Krzysztof Gibasiewicz,*,†,‡ Anna Szrajner,† Janne A. Ihalainen,†,§ Marta Germano,† Jan P. Dekker,† and Rienk van Grondelle†

Department of Physics and Astronomy, Vrije Universiteit, De Boelelaan 1081, 1081 HV Amsterdam, The Netherlands, and Department of Physics, Adam Mickiewicz University, ul. Umultowska 85, 61-614 Poznań, Poland

Received: June 9, 2005; In Final Form: August 26, 2005

Almost all photosystem I (PSI) complexes from oxygenic photosynthetic organisms contain chlorophylls that absorb at longer wavelength than that of the primary electron donor P700. We demonstrate here that the low-energy pool of chlorophylls in the PSI-LHCI complex from the green alga *Chlamydomonas reinhardtii*, containing five to six pigments, is significantly blue-shifted (A_{max} at 700 nm at 4 K) compared to that in the PSI core preparations from several species of cyanobacteria and in PSI-LHCI particles from higher plants. This makes them almost isoenergetic with the primary donor. However, they keep the other characteristic features of "red" chlorophylls: clear spectral separation from the bulk chlorophylls, big Stokes shift revealing pronounced electron−phonon coupling, and large homogeneous and inhomogeneous broadening of ∼170 and ∼310 cm^{-1}, respectively.

Introduction

Photosystem I (PSI) preparations from various species show significant absorption at wavelengths longer than that for the main Q_y band of bulk chlorophylls (Chls) and the primary electron donor, P700. The processes of energy equilibration between these low-energy Chls and bulk Chls were extensively studied (see reviews[1,2]), but the nature, location, and function of these red Chls are still not fully understood.[3−12]

The red forms of Chls were characterized in detail for PSI core complexes from several species of cyanobacteria. At 6 K, two spectral pools of these Chls were identified with steady-state absorption/fluorescence line narrowing techniques: one with absorption maximum at 703 nm (C703, *Synechococcus* PCC 7942) or 708 nm (C708; *Synechocystis* PCC 6803, *Thermosynechococcus elongatus* (*T. elongatus*), *Spirulina platensis* (*S. platensis*)) and the other one with absorption maximum at 719 nm (*T. elongatus*) or at 740 nm (*S. platensis*).[1,13,14] Upon raising the temperature from 6 K to room temperature, the absorption maxima of these pools shift to shorter wavelengths. Emission at 6 K from red Chls is characterized by a large Stokes shift of ∼12 nm for the former pool and of 11−20 nm for the latter pool. The total number of the red Chls per reaction center (RC) was estimated to be 2−10, depending on the species and the state of the PSI core particles (monomeric vs trimeric). Additional red Chls pools at 714−715 nm were reported for PSI cores from *Synechocystis* PCC 6803 and *T. elongatus* on the basis of hole burning spectroscopy.[9,15,16]

Several pools of red Chls were observed in PSI-LHCI complexes from green plants.[4,17] The lowest energy Chls are located in the peripheral antenna, LHCI.[17−20] At 6 K, the maximum of the absorption band of all long-wavelength pigments in PSI-LHCI was estimated to be at 716 nm, whereas the corresponding fluorescence maximum is at 733 nm.[4] In the case of isolated LHCI the absorption band of the corresponding red Chls was estimated to be around 711 nm.[19]

The Stokes shift of "normal" Chls (bulk Chls in photosystems) is only about 1−4 nm[21,22] (also our own unpublished results), much smaller than those observed for the red Chls. This difference was explained by strong pigment−pigment interactions and a mixing of the excited state with a charge transfer state in the case of red Chls.[4,17,23] These effects lead to a significant shift of the potential energy surface of the excited state (high values of Huang−Rhys factors), which results in a coupling of optical transitions to a distribution of phonons of higher energies. Another result of this coupling is a significant homogeneous broadening of the absorption and emission bands of red Chls. The charge-transfer character of the excited states of red Chls[23] also explain the strong modulation of the electronic transition energies by small changes in the protein environment, observed as a large inhomogeneous broadening of the absorption spectra of red Chls.[24]

Unlike PSI preparations from cyanobacteria and higher plants, spectroscopic properties of the PSI from the green alga *Chlamydomonas reinhardtii* (*C. reinhardtii*), the third model PSI system, have rarely been studied and, in particular, detailed spectral properties of red Chl pools have not been reported. This may be because there are no clear separate bands of red Chls visible in the steady-state absorption spectra. Bassi et al.[25] and Kargul et al.[26] reported 77-K emission from the peripheral PSI antenna, LHCI, and the PSI-LHCI supercomplex with maxima at 705 and 715 nm, respectively. In a recent paper, the respective maxima were observed at 708 and 712 nm.[27] Temperature-dependent kinetics of fluorescence decay in whole cells (containing PSI-LHCI) and isolated PSI cores from *C. reinhardtii* were analyzed with a model suggesting the presence of one to two red Chls absorbing at ∼703 nm and located close to

* Corresponding author. E-mail: krzyszgi@amu.edu.pl.
† Vrije Universiteit.
‡ Adam Mickiewicz University.
§ Present address: Institute of Physical Chemistry, University of Zurich, Winterthurerstrasse 190, 8057 Zurich, Switzerland.

10.1021/jp0530909 CCC: $30.25
Published on Web 10/15/2005

the RC.[28,29] These results suggest that the red Chls of the PSI core complex of *C. reinhardtii* resemble those of *Synechococcus* PCC 7942 (which absorb and emit at about 703 and 713 nm, respectively[14]) and that the red Chls of the peripheral antenna absorb and emit considerably more to the blue than the red-most LHCI Chls of green plants.[20] Another motivation to this work came from our earlier observation of excitonic coupling between Chls involved in primary electron transfer in PSI from *C. reinhardtii*. This coupling was proposed to be observable due to the lack of red antenna Chls in the PSI core spectrally overlapping with electron-transfer Chls in this species.[30−32]

In this contribution we applied site-selective (polarized) fluorescence spectroscopy[4] to characterize spectral properties of low-energy Chls in high-quality PSI-LHCI preparations from *C. reinhardtii*. Following a relatively simple modeling, this technique offers an access to parameters of the red Chl pool, such as absorption maximum, Stokes' shift, and ratio of homogeneous and inhomogeneous broadening, and allows conclusions on the electron−phonon coupling of the red Chls in this system.

Materials and Methods

Sample. PSI-LHCI complexes were obtained from *C. reinhardtii* strain CC-2137 by β-DM solubilization and sucrose gradient centrifugation as described in Germano et al.[33] with an additional FPLC run through a Superdex 200 column after the ultracentrifugation. This preparation was characterized before by electron microscopy[33] and consists of two slightly different types of particles which however contain the same number of LHCI subunits.[34] These types of complexes bind most likely 9 LHCI subunits per PSI core complex[35] and contain about 230 Chls (M. Hippler, personal communication; ref 26). The OD of the sample at the maximum of Q_y absorption band (at ∼679 nm) was ∼0.7 cm^{-1} for the absorption measurements, ∼0.11 cm^{-1} for the self-absorption-free fluorescence experiments, and ∼5.5 cm^{-1} for polarized experiments, the high OD being applied in order to improve the signal-to-noise ratio of the collected spectra and calculate anisotropy precisely. The samples were diluted to the proper concentrations in a buffer containing 0.06% β-DM, 20 mM Bis-Tris (pH 6.0), 10 mM NaCl, 5 mM $CaCl_2$, and 60% glycerol (v/v).

Methods. All measurements were done on sample in a 1-cm thick cuvette placed in liquid helium cryostat (Utreks, Ukraine). Absorption spectra were measured on the home-built spectrophotometer.[36] Fluorescence emission spectra were measured with a cooled CCD camera (Chromex ChromCam) equipped with a $^1/_2$-m spectrograph (Chromex 500IS), and corrected for the spectral and light-polarization sensitivity of the detection system. The source of nonselective excitation light at ∼420 nm was a 150-W tungsten halogen lamp equipped with an interference filter (fwhm ∼ 20 nm). Selective excitation at wavelengths ranging from 675 to 726 nm was realized by a continuous wave (cw) dye laser (Coherent CR599), pumped by an argon ion laser (Coherent Innova 310). The fluorescence was collected with 0.4-nm spectral resolution at the angle of 90° to the direction of the excitation beam. Polarization of the excitation light was vertical. The emission light was passing through a polarizer (set vertically or horizontally) before detection or was collected without polarizer. Optical anisotropy, r, was calculated from the following expression:

$$r(\lambda) = [I^{||}(\lambda) - I^{\perp}(\lambda)]/[I^{||}(\lambda) + 2I^{\perp}(\lambda)] \quad (1)$$

where $I^{||}(\lambda)$ and $I^{\perp}(\lambda)$ are the fluorescence intensities measured with the polarizer set vertically and horizontally, respectively.

Modeling. The modeling was described in detail by Gobets et al.[4] Shortly, it was assumed that the red absorption band of low-energy Chl is a superposition of Gaussian curves (of identical widths) representing absorption spectra of individual spectral forms homogenously broadened due to electron−phonon interaction. Furthermore, the distribution of these spectral forms over the wavelength coordinate, or inhomogeneous broadening, was also assumed to be described by a Gaussian function. The ratio of the widths (fwhm) of these two Gaussians, Γ_h and Γ_i, respectively, can be extracted from the site-selective fluorescence experiment. Due to inhomogeneous contribution to the absorption band of red Chl, fluorescence emission spectra depend on which spectral forms of them are excited; i.e., they are excitation-wavelength-dependent, assuming that individual low-energy species are not connected by excitation energy transfer. Finally, it was assumed that the Stokes shift of all of the spectral forms contributing to the red Chl pool was identical. The calculations based on the above assumptions show that the relationship between the wavelength of the fluorescence emission maximum (λ_{em}) and the excitation wavelength (λ_{ex}) is linear:

$$\lambda_{em}(\lambda_{ex}) = \lambda_{0,em} + s(\lambda_{ex} - \lambda_0) \quad (2)$$

where $\lambda_{0,em}$ is a wavelength of maximum of the total fluorescence emission from whole distribution of red Chls. In practice, it is measured after nonselective excitation which is followed by excitation energy transfer to all spectral forms of red Chls. The slope s relates Γ_h and Γ_i:

$$s = \Gamma_i^2/(\Gamma_i^2 + \Gamma_h^2) = \Gamma_i^2/\Gamma_{tot.}^2 \quad (3)$$

where $\Gamma_{tot.}$ is the fwhm of the entire absorption band. λ_0 stands for the wavelength for which the total absorption band of red Chls has its maximum. As seen from the eq 2, the value of λ_0 can be found as a value of excitation wavelength applied in the red Chl region for which $\lambda_{em} = \lambda_{0,em}$. Thus, both s and λ_0 can be found from the experimentally measurable curve $\lambda_{em}(\lambda_{ex})$. The Stokes shift, δ, of the total red Chl pool and all individual spectral forms from this pool is given by the expression:

$$\delta = \lambda_{0,em} - \lambda_0 \quad (4)$$

Results

Absorption and Nonselective Fluorescence Emission Spectra. The absorption spectrum of the PSI-LHCI complex from *C. reinhardtii* at 7 K is shown in Figure 1. It is dominated by the Q_y band of bulk Chl *a* peaking at ∼679 nm. At longer wavelengths, there is a significant tail with two small bumps superimposed at ∼697 and ∼702 nm, which suggest contributions from slightly red-shifted pools of Chls. The fluorescence emission spectrum recorded after nonselective excitation at 420 nm at 4 K (Figure 1) peaks at 712.6 nm ($OD_{679nm} = 0.11$ cm^{-1}), 33 nm to the red compared to the Q_y absorption band from bulk Chls. This huge shift indicates that the source of the emission at 4 K is the low-energy Chls and not bulk Chls. It was found that increasing the OD_{679nm} from 0.11 to 5.5 cm^{-1} results in a shift of the fluorescence emission peak to ∼715 nm due to self-absorption and reemission from the lower energy Chls.

The temperature dependence of the emission spectra between 4 and 214 K is presented in Figure 2. The spectrum at 4 K shows a minor bump at ∼703 nm (clearly seen on the second-derivative graph and not observed at higher temperatures), indicating a separate pool of low-energy Chls trapping the excitations. This wavelength is close to 705 nm where the 77

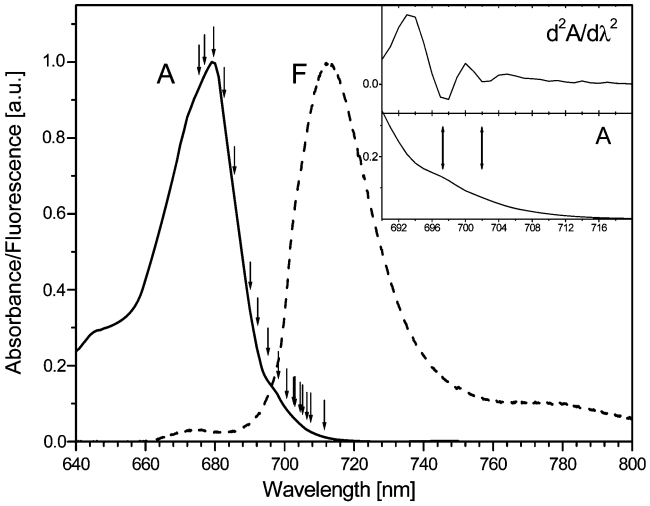

Figure 1. Steady-state absorption spectrum at 7 K (solid) and fluorescence emission spectrum at 4 K (dashed; excitation at 420 nm) of PSI-LHCI particles from *C. reinhardtii*. Arrows indicate excitation wavelengths applied in site-selective fluorescence experiment under self-absorption-free conditions. Lower inset: long-wavelength tail of the absorption spectrum with double arrows indicating positions of two bumps, at ~697 and ~702 nm, which are better seen in the second derivative of the absorption spectrum (upper inset).

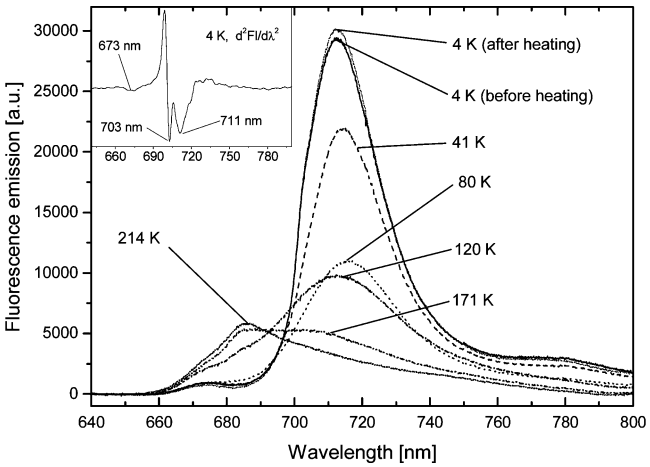

Figure 2. Fluorescence emission spectra of PSI-LHCI particles from *C. reinhardtii* following nonselective excitation at 420 nm at different temperatures. $OD_{679nm,RT} = 0.11\ cm^{-1}$. Inset: second derivative of the fluorescence spectrum at 4 K. The relative integrated intensities for increasing temperatures are respectively: 1.00, 0.79, 0.48, 0.53, 0.34, and 0.29. The fluorescence peak position shifts from 712.6 nm at 4 K to 714.3, 715.8, and 712.8 nm at 41, 80, and 120 K, respectively.

K fluorescence from *C. reinhardtii* LHCI was observed[25] and to 701−702 nm where plant Lhca2 emits at ≤77 K.[37,38] A very small band at ~673 nm is temperature-independent. Therefore it is attributed to a very small fraction of Chls that are not able to transfer the excitation energy to the low-energy Chls emitting at ~712.6 and ~703 nm. We conclude that the bulk Chls are very well coupled to the red Chls. At higher temperatures the fluorescence intensity decreases. This indicates an increasing efficiency of excitation quenching by the reaction center. Between 4 and 80 K the fluorescence maximum position shifts from 712.6 to 715.8 nm, showing that the higher energy red Chls contributing to the blue slope of the fluorescence band transfer the excitation energy to the reaction center more efficiently than the red-most forms. The emission wavelength of 715.8 nm at 80 K agrees better with emission at 715 than at 712 nm reported by Kargul at al.[26] and Takahashi et al.,[27] respectively, for the same type of preparation at 77 K. We have

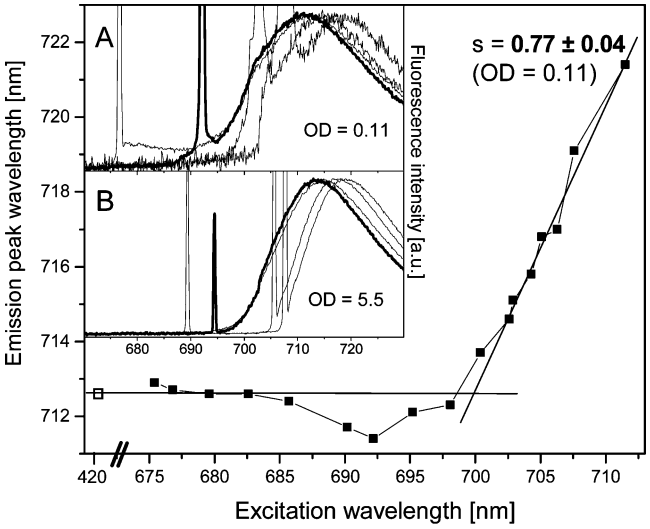

Figure 3. Fluorescence emission peak position as a function of excitation wavelength for PSI-LHCI from *C. reinhardtii* at 4 K. $OD_{679nm,RT} = 0.11\ cm^{-1}$. *s* stands for slope calculated for the low-energy Chl excited selectively at wavelengths > 700 nm. Wavelength of the crossing point of the two straight lines, 700 nm, determines the position of the absorption maximum of the red Chl pool as described in Material and Methods. Closed squares, for site selective excitations; open square, for nonselective excitation at 420 nm (from Figures 1 and 2). Insets A and B: a few representative selective fluorescence spectra for low- and high-concentrated samples (excitation vs emission peak wavelengths are 676.8/712.7, 692.2/711.4, 702.9/715.1, and 707.6/719.1 nm for $OD_{679nm,RT} = 0.11\ cm^{-1}$ and 689.4/714.9, 694.4/714.0, 705.6/717.6, and 707.7/719.1 nm for $OD_{679nm,RT} = 5.5\ cm^{-1}$). For both concentrations, with increasing excitation wavelengths, the emission peak shifts first toward the blue (examples of such spectra are drawn with thick lines in insets) and then toward the red. The narrow lines in the blue parts of the spectra are light-scattering artifacts at excitation wavelengths.

no satisfactory explanation for the small differences in the fluorescence maximum position in these reports, but it should be noted that both the isolation procedures and strains were different in all these studies. A further increase of the temperature leads to an almost complete disappearance of the fluorescence at ~712.6 nm and the buildup of a fluorescence band at 685 nm. The increase of the fluorescence at 685 nm may come from Chls, which are well-coupled to the red Chls but are not effective in excitation energy transfer to the reaction center, at least below 214 K.

Selective Fluorescence Spectra. Application of a spectrally narrow, tunable laser beam allows selective excitation of different spectral forms of Chl *a* contributing to the Q_y absorption band (Figure 1). Selective excitation at wavelengths shorter than ~685 nm leads to emission spectra virtually identical with that one measured at 420-nm excitation, all peaking at ~712.6 nm (for very diluted samples). A further increase of the excitation wavelength leads to emission spectra which are excitation-wavelength-dependent. First, the maximum of the fluorescence emission shifts toward the blue to ~711.4 nm, and then systematically shifts toward the red (Figure 3). The same behavior is maintained for very concentrated samples although, due to self-absorption and reemission, emission wavelengths are shifted up to 2.5 nm toward the red (Figure 3, inset B).

To check if the excitation wavelength dependence of the emission spectra is correlated with the capability of excitation energy transfer between directly excited Chls and their neighbors, we have measured polarized fluorescence emission spectra. For that, the polarization of the exciting light was set vertical,

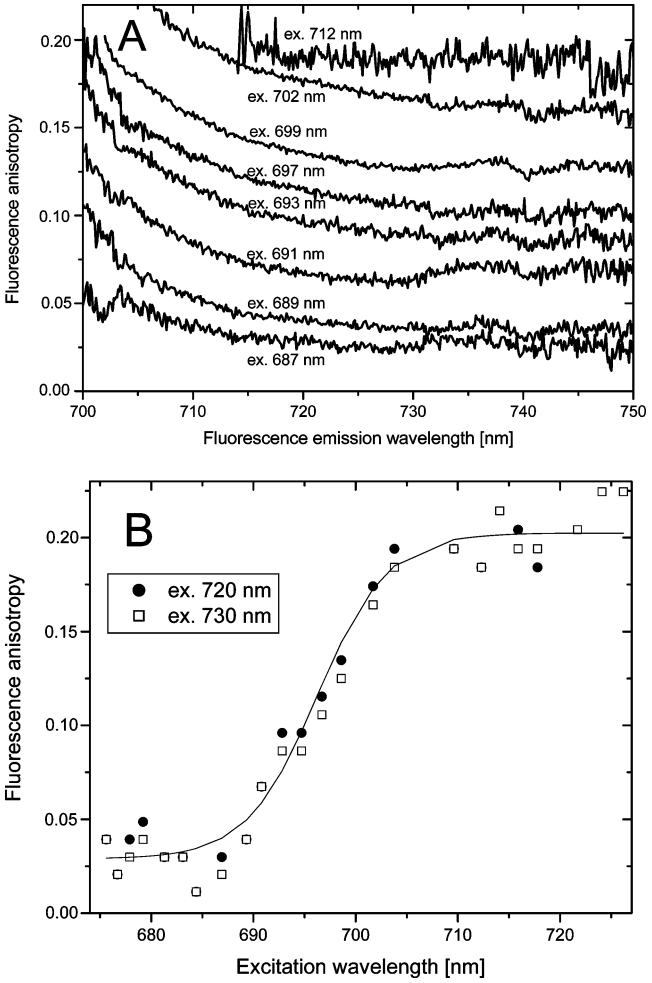

Figure 4. Fluorescence emission anisotropy at ~5K calculated for PSI-LHCI from *C. reinhardtii* ($OD_{679nm,RT} = 5.5\ cm^{-1}$). A, anisotropy shown as a function of detection wavelength for a few selected excitation wavelengths. B, anisotropy calculated at 720 and 730 nm as a function of excitation wavelength. Symbols are the experimental points and the solid line is a sigmoidal fit.

and two components of the emitted light were measured: polarized vertically and horizontally. Based on these data, an optical anisotropy was calculated, as described in Materials and Methods, for the whole set of excitation wavelengths and the whole range of detection wavelengths (Figure 4). For that experiment, the $OD_{679nm,RT}$ of the sample was increased to 5.5 cm^{-1} in order to improve the signal-to-noise ratio. From Figure 4B, it can be seen that the anisotropy is constant and close to zero at shorter excitation wavelengths and starts to rise at about 685−690 nm. This wavelength range fits perfectly the starting point for the excitation-wavelengths dependence of the emission spectra (Figure 3). The anisotropy reaches its maximal value at ~700−705 nm and remains constant above this wavelength, which again correlates well with the point where the emission vs excitation-wavelength dependence starts to be linear. Due to the high concentration of the sample in this experiment, leading to self-absorption and reemission of light, fluorescence anisotropy starts to increase and reaches its maximal value at wavelengths somewhat longer than in low-concentrated samples. However, this shift is expected to be a few nanometers at most, regarding the 2.5-nm shift between emission peak positions of low- and high-concentrated samples (see above).

The correlations between the curves shown in Figures 3 and 4B allow an interpretation of the underlying processes. The excitation energy can be transferred between Chls when exciting

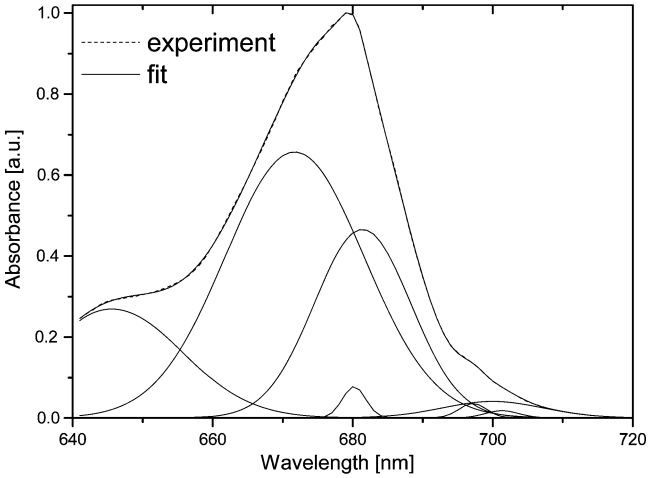

Figure 5. Gaussian decomposition of the 7-K absorption spectrum of PSI-LHCI from *C. reinhardtii*. Parameters of the Gaussians (absorption maximum/full width at half-maximum/relative area under the curve/corresponding number of Chls): 701.3 nm/5.6 nm/0.41%/0.7 Chl; 700.0 nm/17.0 nm (350 cm^{-1})/2.8%/4.9 Chl; 697.2 nm/4.6 nm/0.67%/1.2 Chl; 681.4 nm/16.3 nm/31.3%/55 Chl; 680.2 nm/3.9 nm/1.25%/2 Chl; 671.7 nm/23.4 nm/63.5%/111 Chl; 645.7 nm/23.4 nm. The area under the Chl *b*/vibrational Chl *a* band at 645.7 nm was not taken into account when calculating the relative area of the other bands. The total amount of Chl *a* was assumed to be 175 (Kargul et al.[26]).

below 685−690 nm and is either quenched by the RC or trapped by all spectral forms of red Chls contributing to the inhomogeneously broad pool emitting on average at ~712.6 nm. Systematic tuning of the laser to wavelengths longer than 685 nm leads to increasingly selective excitation of relatively short-wavelength nontransferring red Chls, and therefore the fluorescence peak shifts to shorter wavelengths and a rise of anisotropy is observed. Further tuning of the laser toward the red results in selective excitation of more and more red-shifted Chls (emission peak shifts toward the red) accompanied by further limitation of EET between Chls. No more EET occurs when excitation is at >700−705 nm, meaning that the directly excited red pigments do not exchange excitation energy. From the observation of a significant decrease of the emission peak wavelengths for excitation wavelengths between 685 and 697 nm, due to emission by the relatively blue-shifted red Chls, we conclude that the red Chls pool is spectrally clearly separated from the bulk Chls.

The lack of EET between red Chls fulfills one of the assumptions underlying our modeling (see Materials and Methods). The experimentally observed dependence of emission vs excitation wavelength is linear at $\lambda_{ex} > 700$ nm (Figure 3) in agreement with the prediction of the model. From this model, the absorption maximum of the red Chl pool was found to be at ~700 nm (eq 2), and the slope of the linear part of the $\lambda_{em}(\lambda_{ex})$ dependence is 0.77 ± 0.04, corresponding to the ratio of homogeneous and inhomogeneous broadening of $\Gamma_h/\Gamma_i = 0.55 \pm 0.07$ (Figure 3, eq 3). The Stokes' shift of the red Chls is ~13 nm (eq 4).

Using the value of 700 nm for the absorption maximum of the red Chls pool as the only constraint (see above), the red part of the 7-K absorption spectrum of PSI-LHCI from *C. reinhardtii* was fitted with a sum of seven Gaussian curves: three Gaussians were used for the red Chls, three for bulk Chls, and one for the Chl *b*/vibrational band of Chl *a* (Figure 5). Our primary intention was to get a good fit in the red Chls region, and we do not attribute much significance to the number and parameters of the Gaussian curves in the remaining part of the spectrum. In addition to the dominating 700-nm band we had

TABLE 1: Comparison of Spectral Characteristics of the Low-Energy Chls at ~5 K in Five Different Species[a]

	Synechocystis PCC 6803 Gobets et al.[4]	*Synechococcuss* PCC 7942 Andrizhiyevskaya et al.[14]	spinach Gobets et al.[4]	*Arabidopsis thaliana* Ihalainen et al.[17]	*C. reinhardtii* CC 2137 this work
no. of Chls per RC	~100 (PSI)	~100 (PSI)	~175 (PSI-LHCI)	~175 (PSI-LHCI)	~230 (PSI-LHCI)
λ_0 (nm)[b]	708	703	716	711	700
δ (nm)	10 (12[c])	10	17	23	13
no. of red Chls	2 (3−5[c])	2			5
Γ_i (cm^{-1})	215		360	389	310
Γ_h (cm^{-1})	170		200	130	170
$\Gamma_{tot.}$ (cm^{-1})	270		410		350
Γ_h/Γ_i	0.79		0.55		0.55
s	0.6		0.77		0.77

[a] See text for details. [b] λ_0, absorption maximum of red Chls pool; δ, Stokes shift; Γ_i, inhomogeneous broadening; Γ_h, homogeneous broadening; $\Gamma_{tot.}$, total broadening; *s*, slope. [c] According to Gobets et al.[13] and Gobets and van Grondelle.[1]

to introduce two more relatively narrow Gaussians in the red tail region in order to improve the fit significantly. The maxima of these two Chl pools were found to be at ~697 and ~701 nm, in line with the second-derivative analysis shown in Figure 1, and their oscillator strengths correspond to ~1 Chl each. The width of the 700-nm pool was found to be 350 cm^{-1} (17.0 nm; fwhm), and its oscillator strength corresponded to 5 Chls, assuming 175 Chls *a* per PSI-LHCI.[26]

Discussion

On the basis of the total width of the red Chls pool (centered at 700 nm and labeled C700 from now on) found from the Gaussian decomposition (Figure 5) and the ratio of Γ_h/Γ_i in this pool found from the site-selective experiment (Figure 3, eq 3), the homogeneous and inhomogeneous broadening of low-energy Chls was calculated to be 170 ± 20 and 310 ± 20 cm^{-1}, respectively. These values should be compared to those reported for red Chls from other species and obtained with the same method (Table 1). The homogeneous broadening is almost the same as the one proposed for the C708 pool of the PSI core from *Synechocystis* PCC 6803 and the C716 pool of the PSI-LHCI complex from spinach[4] and only somewhat larger than that for the C711 pool of LHCI in the PSI-LHCI complex from *A. thaliana*.[17] At the same time, the Stokes shift of C700, ~13 nm, is only slightly bigger than that for the C703/C708 pools in cyanobacterial PSI (10−12 nm) but smaller than those in plant PSI-LHCI (17−23 nm). These observations indicate that the distribution of phonons coupled to the 0−0 optical transition is similar for the C700 pool of *C. reinhardtii* and C703/C708 pools of cyanobacterial PSI, but different from the one in LHCI from green plants. This difference results most likely from the higher value of the Huang−Rhys factor in the case of red Chls in LHCI from green plants (2.9)[17] than in the case of C700/C703/C708 pools of the PSI core complexes from cyanobacteria and PSI-LHCI from *C. reinhardtii*. On the basis of the Stokes shifts, one would expect the Huang−Rhys factor of ~1.5 (the value of 2.1 has been modeled for C700; J.A.I., unpublished results) for the C700/C703/C708 pools assuming similar phonon frequency, of the order of 100 cm^{-1}, as in green plants (Stokes shift is proportional to the Huang−Rhys factor and the mean phonon frequency). The similar phonon frequencies in all these systems are suggested by similar homogeneous broadening. The similarity of electron−phonon coupling features in the C700/C703/C708 pools indicates the same nature of low-energy species in PSI-LHCI from *C. reinhardtii* and PSI from *Synechocystis* and *Synechococcus* PCC 7942.

Our results indicate that the inhomogeneous broadening in PSI-LHCI from *C. reinhardtii*, 310 cm^{-1} is significantly bigger than in PSI from *Synechocystis* PCC 6803 (215 cm^{-1}, Table 1). This may be caused by the higher amount of Chls contributing to the red Chl pool in *C. reinhardtii* (5−6 vs 2−5), which implies a broader range of different protein environments tuning electronic transitions in Chls. An alternative explanation could be a somewhat stronger charge-transfer character of the excited state of C700 than of C708. Inhomogeneous broadening is even bigger in PSI-LHCI complex from green plants (360−390 cm^{-1}, Table 1), but this may be because several spectrally overlapping pools of red Chls coexist there.[4,17] Indeed, at least four red Chl pools were reported: two for LHCI[20] and two for PSI core.[17]

It should be emphasized that the spectral parameters obtained and discussed in this contribution cannot be directly compared to those obtained from hole-burning spectroscopy[9,15,16] since it was shown that these two techniques may look selectively at different pools of red Chls in the PSI-LHCI complex.[17] Interestingly, the hole-burning and selective fluorescence studies of red Chls reveal preferentially low-frequency phonons of ~20 cm^{-1} and high-frequency phonons of ~100 cm^{-1}, respectively. In fact, both of these two kinds of phonons are coupled to the optical transition of red Chls that was demonstrated in a very elegant way for red Chls of *Synechocystis* PCC 6803[1] and is taken into account in more advanced modeling.[9,15−17] A trace of the ~20 cm^{-1} phonons coupled to the 0−0 transition was also observed by us for the red Chls pool of *C. reinhardtii* (Figure 6).

In addition to the C700 pool in *C. reinhardtii* containing 5 Chls, two more spectrally narrow pools were found from the Gaussian decomposition at ~697 and ~701 nm with the approximate oscillator strength of 1.2 and 0.7 Chls, respectively. The position and the oscillator strength of the former band indicate that it could be attributed to the primary donor, P. A similar band at 697 nm with the oscillator strength of ~2 resulting from Gaussian decomposition was attributed to the primary donor in PSI from *Synechocystis* PCC 6803,[4] *Synechocystis* PCC 7942,[14] and *C. reinhardtii*.[28] The same position of the primary donor absorption in cyanobacteria and *C. reinhardtii* is intriguing because the ($P^+ - P$) difference spectrum from the latter species peaks consistently a few nanometers to the blue relative to cyanobacteria.[30,39−43] A sharp band at 696 nm also was observed in PSI-LHCI from *Arabidospsis* and attributed to pigments in the interfaces between LHCI subunits or between LHCI and PSI.[44] We may speculate that the second pool, at 701 nm, correspond to one to two red Chls located close to the RC as reported for *C. reinhardtii*.[28,29] The sharp character of the 697- and 701-nm bands may indicate that the mechanism of their red shift is different from the C700 pool: for example that they originate from monomeric Chls which are tuned by the protein environment.[11]

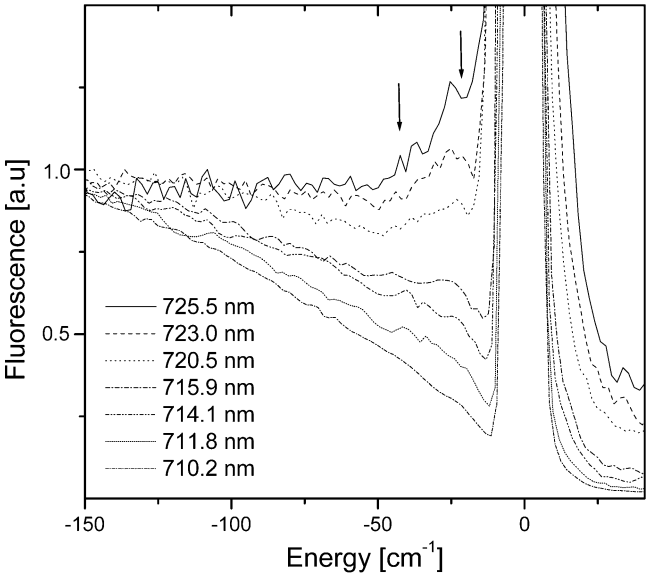

Figure 6. Site-selective nonpolarized fluorescence spectra from PSI-LHCI of *C. reinhardtii* recorded at ~5K at seven representative excitation wavelengths (given in the legend) and shifted along the energy axis in such a way that excitation wavelength coincides with energy 0 cm^{-1}. The arrows separated 21.5 cm^{-1} from each other and from the point of zero energy indicate progression of two phonons. $OD_{679nm,RT} = 5.5$ cm^{-1}.

As seen from Figure 5, the profiles of the 697- and 701-nm pools are superimposed on the 700-nm pool of red Chls. However, these two small pools are not expected to introduce any important modifications to the applied model. If the 697-nm pool is due to the primary donor, it is not expected to contribute at all to the low-temperature fluorescence spectra due to immediate quenching by charge separation. Since the 701-nm pool is relatively small and sharp, its contribution to the low-temperature emission, especially following excitation in the red slope of the broad C700 pool, should be negligible.

Our results do not definitely answer the question about the localization of the C700 pool. However, previous observations of a high degree of similarity between PSI core complexes from different organisms (an impressing similarity was shown recently for PSI from the cyanobacterium *T. elongatus*[8] and higher plants[45]), together with our observation of spectral similarities between C700 and cyanobacterial C703 and C708 pools indicate that C700 is located in the PSI core. The number of ~5 Chls in C700, which is slightly more than the number of Chls in C703 and C708, suggests further that it may be contributed by two to three Chl dimers (or a dimer plus trimer), one to two of them not having a counterpart in cyanobacterial PSI. This extra dimer(s) may possibly be located in the interface between LHCI and the PSI core, but probably not within LHCI, from which a shorter wavelength fluorescence was reported[25,27] than from PSI-LHCI. A distant location from the RC of a fraction of the low-energy Chls is suggested by the presence of emission at 685 nm at 214 K (Figure 2) coming from Chls which are in contact with red pigments but are not quenched by RC.

Acknowledgment. K.G. gratefully acknowledges a Marie-Curie Individual Fellowship, Contract HPMF-CT-2002-01812, a NWO grant (B 81-734), and the Access to Research Infrastructures activity in the Sixth Framework Program of the EU (Contract RII3-CT-2003-506350, Laserlab Europe). J.A.I. was funded by the European Community's Human Potential Program Grant HPRN-CT-2002-00248 (PSICO). J.A.I. is grateful for a grant by the Academy of Finland, Project No. 203824.

References and Notes

(1) Gobets, B.; van Grondelle, R. *Biochim. Biophys. Acta* **2001**, *1507*, 80.

(2) Melkozernov, A. N. *Photosynth. Res.* **2001**, *70*, 129.

(3) Trissl, H.-W.; Wilhelm, C. *Trends Biochem. Sci.* **1993**, *18*, 415.

(4) Gobets, B.; van Amerongen, H.; Monshouwer, R.; Kruip, Y.; Rögner, M.; van Grondelle, R.; Dekker, J. P. *Biochim. Biophys. Acta* **1994**, *1188*, 75.

(5) Karapetyan, N. V.; Holzwarth, A. R.; Rögner, M. *FEBS Lett.* **1999**, *460*, 395.

(6) Rivadossi, A.; Zucchelli, G.; Garlaschi, F. M.; Jennings, R. C. *Photosynth. Res.* **1999**, *60*, 209.

(7) Engelmann, E.; Tagliabue, T.; Karapetyan, N. V.; Garlaschi, F. M.; Zucchelli, G.; Jennings, R. C. *FEBS Lett.* **2001**, *499*, 112.

(8) Jordan, P.; Fromme, P.; Witt, H. T.; Klukas, O.; Saenger, W.; Krauss, N. *Nature* **2001**, *411*, 909.

(9) Zazubovich, V.; Matsuzaki, S.; Johnson, T. W.; Hayes, J. M.; Chitnis, P. R.; Small, G. *J. Chem. Phys.* **2002**, *275*, 47.

(10) Damjanovic, A.; Vaswani, H. M.; Fromme, P.; Fleming, G. R. *J. Phys. Chem. B* **2002**, *106*, 10251.

(11) Byrdin, M.; Jordan, P.; Krauss, N.; Fromme, P.; Stehlik, D.; Schlodder, E. *Biophys. J.* **2002**, *83*, 433.

(12) Yang, M.; Damjanovic, A.; Vaswani, H. M.; Fleming, G. R. *Biophys. J.* **2003**, *85*, 140.

(13) Gobets, B.; van Stokkum, I. H. M.; Rögner, M.; Kruip, J.; Schlodder, E.; Karapetyan, N. V.; Dekker, J. P.; van Grondelle, R. *Biophys. J.* **2001**, *81*, 407.

(14) Andrizhiyevskaya, E. G.; Schwabe, T. M. E.; Germano, M.; D'Haene, S.; Kruip, J.; van Grondelle, R.; Dekker, J. P. *Biochim. Biophys. Acta* **2002**, *1556*, 265.

(15) Rätsep, M.; Johnson, T. W.; Chitnis, P. R.; Small, G. J. *J. Phys. Chem. B* **2000**, *104*, 836.

(16) Hayes, J. M.; Matsuzaki, S.; Rätsep, M.; Small, G. J. *J. Phys. Chem. B* **2000**, *104*, 5625.

(17) Ihalainen, J. A.; Rätsep, M.; Jensen, P. E.; Scheller, H. V.; Croce, R.; Bassi, R.; Korppi-Tommola, J. E. I.; Freiberg, A. *J. Phys. Chem. B* **2003**, *107*, 9086.

(18) Croce, R.; Zucchelli, G.; Garlaschi, F. M.; Jennings, R. C. *Biochemistry* **1998**, *37*, 17355.

(19) Ihalainen, J. A.; Gobets, B.; Sznee, K.; Brazzoli, M.; Croce, R.; Bassi, R.; van Grondelle, R.; Korppi-Tommola, J. E. I.; Dekker, J. P. *Biochemistry* **2000**, *39*, 8625.

(20) Morosinotto, T.; Breton, J.; Bassi, R.; Croce, R. *J. Biol. Chem.* **2003**, *278*, 49223.

(21) Gillie, J. K.; Lyle, P. A.; Small, G. J.; Golbeck, J. H. *Photosynth. Res.* **1989**, *22*, 233.

(22) Kwa, S. L. S.; Volker, S.; Tilly, N. T.; van Grondelle, R.; Dekker, J. P. *Photochem. Photobiol.* **1994**, *59* (2), 219.

(23) Frese, R. N.; Palacios, M. A.; Azzizi, A.; van Stokkum, I. H. M.; Kruip, J.; Rögner, M.; Karapetyan, N. V.; Schlodder, E.; van Grondelle, R.; Dekker, J. P. *Biochim. Biophys. Acta* **2002**, *1554*, 180.

(24) Renger, T. *Phys. Rev. Lett.* **2004**, *93*, 188101.

(25) Bassi, R.; Soen, S. Y.; Frank, G.; Zuber, H.; Rochaix, J.-D. *J. Biol. Chem.* **1992**, *267*, 25714.

(26) Kargul, J.; Nield, J.; Barber, J. *J. Biol. Chem.* **2003**, *278*, 16135.

(27) Takahashi, Y.; Yasui, T.; Stauber, E. J.; Hippler, M. *Biochemistry* **2004**, *43*, 7816.

(28) Jia, Y.; Jean, J. M.; Werst, M. M.; Chan, C.-K.; Fleming, G. R. *Biophys. J.* **1992**, *63*, 259.

(29) Werst, M.; Jia, Y.; Mets, L.; Fleming, G. R. *Biophys. J.* **1992**, *61*, 868.

(30) Gibasiewicz, K.; Ramesh, V. M.; Melkozernov, A. N.; Lin, S.; Woodbury, N. W.; Blankenship, R. E.; Webber, A. N. *J. Phys. Chem. B* **2001**, *105*, 11498.

(31) Gibasiewicz, K.; Ramesh, V. M.; Lin, S.; Woodbury, N. W.; Webber, A. N. *J. Phys. Chem. B* **2002**, *106*, 6322.

(32) Gibasiewicz, K.; Ramesh, V. M.; Lin, S.; Redding, K.; Woodbury, N. W.; Webber, A. N. *Biophys. J.* **2003**, *85*, 2547.

(33) Germano, M.; Yakushevska, A. E.; Keegstra, W.; van Gorkom, H. J.; Dekker, J. P.; Boekema, E. J. *FEBS Lett.* **2002**, *525*, 121.

(34) Dekker, J. P.; Boekema, E. J. *Biochim. Biophys. Acta* **2005**, *1706*, 12.

(35) Stauber, E. J.; Fink, A.; Markert, C.; Kruse, O.; Johanningmeier, U.; Hippler, M. *Eukaryotic Cell* **2003**, *2* (5), 978.

(36) Pålsson, L.-O.; Flemming, C.; Gobets, B.; van Grondelle, R.; Dekker, J. P.; Schlodder, E. *Biophys. J.* **1998**, *74*, 2611.

(37) Castelletti, S.; Morosinotto, T.; Robert, B.; Caffarri, S.; Bassi, R.; Croce, R. *Biochemistry* **2003**, *42*, 4226.

(38) Croce, R.; Morosinotto, T.; Ihalainen, J. A.; Chojnicka, A.; Breton, J.; Dekker, J. P.; van Grondelle, R.; Bassi, R. *J. Biol. Chem*. **2004**, *279*, 48543.

(39) Melkozernov, A. N.; Su, H.; Lin, S.; Bingham, S.; Webber, A. N.; Blankenship, R. E. *Biochemistry* **1997**, *36*, 2898.

(40) Melkozernov, A. N.; Lin, S.; Blankenship, R. E. *Biochemistry* **2000**, *39*, 1489.

(41) Krabben, L.; Schlodder, E.; Jordan, R.; Carbonera, D.; Giacometti, G.; Lee, H.; Webber, A. N.; Lubitz, W. *Biochemistry* **2000**, *39*, 13012.

(42) Savikhin, S.; Xu, W.; Chitnis, P. R.; Struve, W. S. *Biophys. J.* **2000**, *79*, 1573.

(43) Savikhin, S.; Xu, W.; Martinsson, P.; Chitnis, P. R.; Struve, W. S. *Biochemistry* **2001**, *40*, 9282.

(44) Klimmek, F.; Ganeteg, U.; Ihalainen, J. A.; van Roon, H.; Jensen, P. E.; Scheller, H. V.; Dekker, J. P.; Jansson, S. *Biochemistry* **2005**, *44*, 3065.

(45) Ben-Shem, A.; Frolow, F.; Nelson, N. *Nature* **2003**, *426*, 630.